SAND REPORT

SAND2002-3303
Unlimited Release
Printed October 2002

Bursting Frequency Predictions for Compressible Turbulent Boundary Layers

William W. Liou and Yichuan Fang

Prepared by
Sandia National Laboratories
Albuquerque, New Mexico 87185 and Livermore, California 94550

Sandia is a multiprogram laboratory operated by Sandia Corporation,
a Lockheed Martin Company, for the United States Department of
Energy under Contract DE-AC04-94AL85000.

Sandia National Laboratories

Issued by Sandia National Laboratories, operated for the United States Department of Energy by Sandia Corporation.

Printed in the United States of America. This report has been reproduced directly from the best available copy.

Available to DOE and DOE contractors from
U.S. Department of Energy
Office of Scientific and Technical Information
P.O. Box 62
Oak Ridge, TN 37831

Telephone: (865)576-8401
Facsimile: (865)576-5728
E-Mail: reports@adonis.osti.gov
Online ordering: http://www.doe.gov/bridge

Available to the public from
U.S. Department of Commerce
National Technical Information Service
5285 Port Royal Rd
Springfield, VA 22161

Telephone: (800)553-6847
Facsimile: (703)605-6900
E-Mail: orders@ntis.fedworld.gov
Online order: http://www.ntis.gov/ordering.htm

SAND2002-3303
Unlimited Release
Printed October 2002

Bursting Frequency Predictions for Compressible Turbulent Boundary Layers

William W. Liou and Yichuan Fang
Department of Mechanical and Aeronautical Engineering
Western Michigan University
Kalamazoo, MI 49008

Abstract

A computational method for the prediction of the bursting frequency associated with the coherent streamwise structures in high-speed compressible turbulent boundary layers is presented. The structures are described as wavelike disturbances of the turbulent mean flow. A direct resonance theory is used to determine the frequency of bursting. The resulting hydrodynamic linear stability equations are discretized by using a Chebyshev collocation method. A global numerical method capable of resolving the entire eigenvalue spectrum is used. Realistic turbulent mean velocity and temperature profiles are applied. For all of the compressible turbulent boundary layers calculated, the results show at least one frequency that satisfies the resonance condition. A second frequency can be identified for cases with high Reynolds numbers. An estimate is also made for the profile distribution of the temperature disturbance.

Acknowledgement

This is a report of activities performed for Sandia National Laboratories under Contract No. 14335. Roy S. Baty and Don Potter are the technical monitor for this code development project.

Contents

This Page Intentionally Blank

Nomenclature

A	amplitude for temperature fluctuation
C_i	coefficient matrices in equation 16
D_2	lambda matrix of degree two
M	Mach number
N	number of grid points
Re	Reynolds number
T	mean temperature
T_r	wall recover temperature
T'	temperature fluctuation
U	mean x-component of velocity
a	coefficient in equation 9
b	coefficient in equation 9
c	waves peed
i	$\sqrt{-1}$
$k_{\max}$	local maximum turbulent kinetic energy
$\hat{p}$	mode shape for pressure
r	recovery factor
s_p	stretching parameter
$\hat{T}$	mode shape for temperature
$\hat{u}$	mode shape for x-component of velocity
u_τ	friction velocity
$\hat{v}$	mode shape for y-component of velocity
$\hat{w}$	mode shape for z-component of velocity
x	x coordinate
y	y coordinate
z	z coordinate
$\widetilde{f}$	solution vector
$\overline{y}$	transformed y coordinate
ω	dimensionless frequency
ω^*	dimensional frequency
ω^+	$\omega^* \upsilon_{wall} / u_\tau^2$
α	wave number in the x-direction
β	wave number in the z-direction
β^+	$u_\tau / \beta \upsilon_{wall}$
δ	boundary layer thickness
δ^*	boundary layer displacement thickness
η	y-component of vorticity
μ	dynamic viscosity
υ	kinematic viscosity
λ	bulk viscosity
γ	ratio of specific heats

This Page Intentionally Blank

1.0 Introduction

Large-scale coherent structures have been observed in incompressible and compressible turbulent boundary layers. They exist in the near-wall as well as the outer regions and are believed to be responsible for maintaining the turbulence in the boundary layer. Comprehensive reviews of their behaviors can be found in the literature.[1,2] In the near-wall region, alternating streaks of low- and high-speed fluid (relative to the mean) have been observed,[3] supporting a view that counter-rotating streamwise vortices exist very near the wall. The quasi-deterministic occurrence of these large-scale organized structures and the production of turbulence associated with the violent eruption of the near-wall fluid are collectively referred to as the bursting process. The fluid dynamic processes described by the term bursting vary slightly since its first use.[4] It is, nevertheless, generally believed that the bursting process is of critical importance to the development of turbulent boundary layers.

Due to the necessary resolution of scales, experimental results focusing on the near-wall region are primarily limited to low Reynolds numbers and subsonic speeds. The spanwise spacing of the near-wall structures has been reported to be about 100 based on the near-wall viscous length scale by many experiments.[3,5] The frequency of bursting has also been of intense interests. Partly because of the subjective nature of the current experimental methods devised to detect the bursting process, there is less of a consensus regarding the frequency of the bursting process and its scaling.[6] As most of the turbulence production in the boundary layer occurs in the near-wall region,[7] the time scale of the bursting process is dynamically important to further a fundamental understanding of the development of turbulent boundary layers.

The frequency of bursting is of practical interests to high-speed aerospace applications. The dynamics of the boundary layer structures may also be important in the acoustic noise generation and propagation from high-speed engines.

Computational models for the coherent near-wall structures in incompressible turbulent boundary layers have been proposed.[8-10] It has been shown[11] that the statistically dominant streamwise fluctuation exhibits wavelike characteristics, suggesting that a hydrodynamic wave description for the streamwise structures can be applicable. Models based on hydrodynamic stability theory for the coherent structures in both the outer and the near-wall regions of flat-plate boundary layers were reported.[9,10] Jang et al.[8] proposed a direct resonance theory to describe the bursting events. The structures are described as wavelike disturbances of the turbulent mean flow. They argued that, based on a weakly nonlinear analysis, resonance between the vertical velocity and the free mode of the vertical vorticity equations could occur. Using a temporal stability analysis and a shooting method, they have predicted a bursting frequency, nondimensionalized by the viscous scales, of 0.09 for incompressible turbulent boundary layers, which agrees well with experiment data.[11] They have also showed that the secondary mean flow induced by the resonant discrete mode contains streamwise vortical structures. The shape of the predicted structure and the spacing of the accompanying low-speed streaks are comparable to those observed in experiments. The direct resonance model has been applied to examine the more realistic spatially developing disturbances in incompressible turbulent boundary layers.[12] A numerical solver **BURFIT** (**BUR**sting **F**requency Prediction in **I**ncompressible **T**urbulent Boundary Layers) has been developed and described in a Sandia Report SAND2000-0221. The calculated bursting frequency is 0.0962.

Note that a linear analysis has been used, with the calculated turbulent mean velocity profiles as the basic flow, to approximate the local characteristics of the coherent large-scale structures in incompressible turbulent free mixing layers.[13] A three-component decomposition of the flow quantities, same as that used in the present study, equation (1), was applied and a predictive turbulence closure model was developed by describing the dynamics of the large-scale coherent structures with a weakly nonlinear theory. The results show that the calculated mean velocity, the Reynolds shear stress and the dynamic evolution of the structures agree well with experiments. This and the other studies cited above indicate that the instability wave descriptions of the coherent structures are viable models for simple free and bounded shear layers.

In this paper, a computational method for the prediction of the bursting frequency in compressible turbulent boundary layers is presented. The methodology is developed based on an extension of the incompressible direct resonance model[8] to high-speed boundary layers. The result will show that the present compressible formulation predicts the same bursting frequency as that obtained in Liou et al.[12] for incompressible turbulent boundary layers. Therefore, the present formulation is applicable to both incompressible and compressible turbulent boundary layers. It should be noted that it is not an intension here to build a turbulence closure model for the mean flow or the dynamic evolution of the streamwise coherent structures in compressible boundary layers.

It is stated in Morkovin's hypothesis[14] that "the essential dynamics of these shear flows will follow the incompressible pattern" for small fluctuating Mach numbers. In the absence of strong sources of mass and heat, the hypothesis has been found applicable to boundary layers of free stream Mach numbers less than 4 or 5.[2] The hypothesized dynamic similarity between the incompressible and the compressible turbulent boundary layers is invoked in this exploratory application of the direct resonance theory to the compressible regime. Fluid property variations accompanying that of temperature are considered. Note that there may be other compressibility effects that play a role in the near-wall region of supersonic turbulent boundary layers where the flow gradients are large. There is, however, little substantive experimental evidence to support such conjectures.

In the following section, the present compressible formulation of the direct resonance model and the numerical methods used are described. Results are presented for compressible boundary layers with various Reynolds numbers and free stream Mach numbers. A computer code **BURFICT** (**BUR**sting **F**requency Prediction in **I**ncompressible and **C**ompressible **T**urbulent Boundary Layers) contains a Fortran implementation of these methods and the results shown here have been obtained by using BURFICT.

2.0 Formulation

Bursting Mode Frequency

Turbulence quantities, f, are decomposed into three components[8]:

$$f = F + f' + \breve{f} \tag{1}$$

where F represents a long-time average of f, f' the wavelike component of f, and $\breve{f}$ the background fluctuation. Substituting equation (1) into the Navier-Stokes equations, followed by a linearization of the disturbance quantities, the equations governing the mode shapes of the three velocity components, $u,v,w,$ pressure p and temperature T are

$$\frac{\gamma M^2}{T}\hat{p}(-i\omega) - \frac{1}{T^2}\hat{T}(-i\omega) + \frac{1}{T}\hat{u}(i\alpha) + U[\frac{\gamma M^2}{T}\hat{p}(i\alpha) - \frac{1}{T^2}\hat{T}(i\alpha)] + \frac{1}{T}\frac{\mathrm{d}\hat{v}}{\mathrm{d}y} - \frac{1}{T^2}\frac{\mathrm{d}T}{\mathrm{d}y}\hat{v} + \frac{1}{T}\hat{w}(i\beta) = 0 \tag{2a}$$

$$\begin{aligned}
&[\hat{u}(-i\omega) + U\hat{u}(i\alpha) + \hat{v}\frac{\mathrm{d}U}{\mathrm{d}y}]/T = \\
&-\hat{p}(i\alpha) + \frac{\mu}{\mathrm{Re}}\{l_2(-\alpha^2)\hat{u} + l_1[\frac{\mathrm{d}\hat{v}}{\mathrm{d}y}(i\alpha) + \hat{w}(-\alpha\beta)] + \frac{\mathrm{d}^2\hat{u}}{\mathrm{d}y^2} + \hat{u}(-\beta^2) + \frac{1}{\mu}\frac{\mathrm{d}\mu}{\mathrm{d}T}\frac{\mathrm{d}T}{\mathrm{d}y}[\frac{\mathrm{d}\hat{u}}{\mathrm{d}y} + \hat{v}(i\alpha)] \\
&+ \frac{1}{\mu}\frac{\mathrm{d}\mu}{\mathrm{d}T}[\frac{\mathrm{d}^2U}{\mathrm{d}y^2}\hat{T} + \frac{\mathrm{d}U}{\mathrm{d}y}\frac{\mathrm{d}\hat{T}}{\mathrm{d}y}] + \frac{1}{\mu}\frac{\mathrm{d}^2\mu}{\mathrm{d}T^2}\frac{\mathrm{d}T}{\mathrm{d}y}\frac{\mathrm{d}U}{\mathrm{d}y}\hat{T}\}
\end{aligned} \tag{2b}$$

$$\begin{aligned}
&[\hat{v}(-i\omega) + U\hat{v}(i\alpha)]/T = \\
&-\frac{\mathrm{d}\hat{p}}{\mathrm{d}y} + \frac{\mu}{\mathrm{Re}}\{\hat{v}(-\alpha^2) + l_1[\frac{\mathrm{d}\hat{u}}{\mathrm{d}y}(i\alpha) + \frac{\mathrm{d}\hat{w}}{\mathrm{d}y}(i\beta)] + l_2\frac{\mathrm{d}^2\hat{v}}{\mathrm{d}y^2} + \hat{v}(-\beta^2) + \frac{1}{\mu}\frac{\mathrm{d}\mu}{\mathrm{d}T}\frac{\mathrm{d}U}{\mathrm{d}y}\hat{T}(i\alpha) \\
&+ \frac{1}{\mu}\frac{\mathrm{d}\mu}{\mathrm{d}T}\frac{\mathrm{d}T}{\mathrm{d}y}[l_0\hat{u}(i\alpha) + \hat{w}(i\beta)] + l_2\frac{\mathrm{d}\hat{v}}{\mathrm{d}y}\}
\end{aligned} \tag{2c}$$

$$\begin{aligned}
&[\hat{w}(-i\omega) + U\hat{w}(i\alpha)]/T = \\
&-\hat{p}(i\beta) + \frac{\mu}{\mathrm{Re}}\{\hat{w}(-\alpha^2) + l_1[\hat{u}(-\alpha\beta) + \frac{\mathrm{d}\hat{v}}{\mathrm{d}y}(i\beta)] + \frac{\mathrm{d}^2\hat{w}}{\mathrm{d}y^2} + l_2\hat{w}(-\beta^2) + \frac{1}{\mu}\frac{\mathrm{d}\mu}{\mathrm{d}T}\frac{\mathrm{d}T}{\mathrm{d}y}[\hat{v}(i\beta) + \frac{\mathrm{d}\hat{w}}{\mathrm{d}y}]\}
\end{aligned} \tag{2d}$$

$$[\hat{T}(-i\omega)+U\hat{T}(i\alpha)+\hat{v}\frac{\mathrm{d}T}{\mathrm{d}y}]/T=$$
$$(\gamma-1)M^2[\hat{p}(-i\omega)+U\hat{p}(i\alpha)]+\frac{\mu}{\mathrm{Re}\,\mathrm{Pr}}\{\hat{T}(-\alpha^2-\beta^2)+\frac{\mathrm{d}^2\hat{T}}{\mathrm{d}y^2}+\frac{2}{k}\frac{\mathrm{d}k}{\mathrm{d}T}\frac{\mathrm{d}T}{\mathrm{d}y}\frac{\mathrm{d}\hat{T}}{\mathrm{d}y} \tag{2e}$$
$$+[\frac{1}{k}\frac{\mathrm{d}k}{\mathrm{d}T}\frac{\mathrm{d}^2T}{\mathrm{d}y^2}+\frac{1}{k}\frac{\mathrm{d}^2k}{\mathrm{d}T^2}(\frac{\mathrm{d}T}{\mathrm{d}y})^2]\hat{T}\}+(\gamma-1)M^2\frac{\mu}{\mathrm{Re}}\{2\frac{\mathrm{d}U}{\mathrm{d}y}[\frac{\mathrm{d}\hat{u}}{\mathrm{d}y}+\hat{v}(i\alpha)]+\frac{1}{\mu}\frac{\mathrm{d}\mu}{\mathrm{d}T}(\frac{\mathrm{d}U}{\mathrm{d}y})^2\hat{T}\}$$

Equation (2) has been derived by assuming a normal mode solution for spatially developing wavelike disturbances in a locally parallel mean flow, i.e.,

$$(u',v',w',p',T')=[\hat{u}(y),\hat{v}(y),\hat{w}(y),\hat{p}(y),\hat{T}(y)]\exp[i(\alpha x+\beta z-\omega t)] \tag{3}$$

Equation (2) has been nondimensionalized by using the free stream quantities F_∞ and the boundary layer displacement thickness δ^*. In equation (2), U and T represent the streamwise mean velocity and mean temperature in the turbulent boundary layer. $l_j(=j+\lambda/\mu)$ represent constants related to the fluid viscosity, μ and λ. The cross-correlations between the turbulent fluctuations have been neglected because of their assumed disparate time scales. The Reynolds stresses associated with the random background fluctuation are also neglected in the formulation, as the transport processes are assumed predominantly large-scale. Equation (2) governs the mode shapes of the wavelike disturbances *f'* about the mean flow F in terms of the complex streamwise wave number α, the spanwise wave number β, the frequency ω, the flow Mach number M and the Reynolds number Re. With these assumptions, the resulting equations become the linear hydrodynamic stability equations for compressible fluid flows.[15,16]

In this study, the bursting frequency ω of the coherent structures in compressible turbulent boundary layers is sought using the direct resonance model. The condition for direct resonance can be written as,

$$c^{CME}(\alpha,\beta,M,\mathrm{Re})=c^{VV}(\alpha,\beta,M,\mathrm{Re}) \tag{4}$$

where c^{CME} and c^{VV} represent the wave speeds associated with the continuity, momentum and energy equation (CME) and the free mode of the vertical vorticity (VV) eigenvalue problems, respectively. The equation for the vertical vorticity η can be written as

$$[i(\alpha U-\omega)-\frac{T\mu}{\mathrm{Re}}(\frac{\mathrm{d}^2}{\mathrm{d}\,y^2}+\frac{1}{\mu}\frac{\mathrm{d}\,\mu}{\mathrm{d}\,T}\frac{\mathrm{d}\,T}{\mathrm{d}\,y}\frac{\mathrm{d}}{\mathrm{d}\,y}-\alpha^2-\beta^2)]\,\hat{\eta}= \\ -(i\beta)\frac{\mathrm{d}\,U}{\mathrm{d}\,y}\hat{v}+(i\beta)\frac{T}{R}[\,(\frac{\mathrm{d}\,\mu}{\mathrm{d}\,T}\frac{\mathrm{d}^2\,U}{\mathrm{d}\,y^2}+\frac{\mathrm{d}^2\,\mu}{\mathrm{d}\,T^2}\frac{\mathrm{d}U}{\mathrm{d}\,y}\frac{\mathrm{d}\,T}{\mathrm{d}\,y})+\frac{\mathrm{d}\,\mu}{\mathrm{d}\,T}\frac{\mathrm{d}U}{\mathrm{d}\,y}\frac{\mathrm{d}}{\mathrm{d}\,y}\,]\,\hat{T} \tag{5}$$

In this study, the mean velocity and temperature profiles of the turbulent boundary layers have been obtained from the numerical solutions of a Navier-Stokes equation solver.[17] Efforts were taken to ensure convergence in not only the U and T profiles but also their derivatives that were used in the stability equations.

The boundary conditions on the isothermal wall are

$$\hat{u}=\hat{v}=\hat{T}=\hat{w}=0 \tag{6}$$

A wall boundary condition for the pressure disturbance can be obtained by substituting equation (6) into equation (2c). The resulting equation can be written as

$$\frac{\partial\,\hat{p}}{\partial\,y}=\frac{\mu}{R}[l_1(i\alpha\frac{\partial\hat{u}}{\partial\,y}+i\beta\frac{\partial\,\hat{w}}{\partial\,y})]+l_2\,\frac{\partial^2\,\hat{v}}{\partial\,y^2}+\frac{1}{\mu}\frac{\mathrm{d}\,\mu}{\mathrm{d}\,T}\frac{\mathrm{d}\,T}{\mathrm{d}\,y}l_2\,\frac{\partial\hat{v}}{\partial\,y} \tag{7}$$

The boundary conditions at the freestream are that all disturbances vanish at the far field.

Bursting Mode Temperature Fluctuation

The temperature distributions associated with the bursting mode can be obtained by using the following relation,

$$T' = A\,\hat{T}(y)\,\exp[i(\alpha x + \beta z - \omega t)] \tag{8}$$

where A represents an amplitude. An estimate for the local amplitude can be obtained by using the Strong Reynolds Analogy (SRA). The resulting equation becomes,

$$A = T(\gamma - 1)M^2\left(\frac{q/U^2}{1 + a + b}\right) \tag{9}$$

$$q = 2k_{\max} \tag{10}$$

where $k_{\max}$ denotes the local maximum turbulent kinetic energy that can be extracted from the mean equations solver. The energetic bursting of the turbulent structures near the wall are assumed to dominate the events that contribute to the peak turbulent kinetic energy. a and b represent the ratio of the normal and spanwise components of the turbulent kinetic energy to that of the streamwise component, respectively.

3.0 Numerical Methods

Various numerical methods for solving the stability equations like equations (2) and (4) have been used in the literature.[15,16,18-23] In the present study, the equations have been discretized by applying the Chebyshev collocation method.[24] The Gauss-Lobatto collocation points are used in this study.

$$\bar{y}_i = \cos(\pi i / N) \qquad (i = 0, 1, \cdots, N\ ) \tag{11}$$

where N+1 represents the total number of collocation points. The approximated solutions for the disturbances can be written as

$$\hat{f} = \sum_0^N \hat{f}_i \varphi_i(\bar{y}) \tag{12}$$

The approximation simultaneously interpolates the solution at the collocation points. That is,

$$\varphi_i(\bar{y}_j) = \delta_{ij} \tag{13}$$

An algebraic mapping has been applied to map the Chebyshev domain $\bar{y} \in [-1,1]$ to the semi-infinite physical domain, y,

$$y = \frac{y_{\max} s_p (1+\bar{y})}{2s_p + y_{\max}(1-\bar{y})} \tag{14}$$

s_p denotes a stretching parameter. The resulting homogeneous system of equations forms an eigenvalue problem that is nonlinear in the parameter α. For equation (2), it can be written as

$$\mathrm{D}_2(\alpha)\tilde{f} = 0 \tag{15}$$

where $\tilde{f}$ denotes a vector containing the solution variables $(\hat{u}, \hat{v}, \hat{w}, \hat{p}, \hat{T})$ at the collocation points. The matrix D_2 represents a lambda matrix of degree two and can be expressed as a scalar polynomial with matrix coefficients:

$$\mathrm{D}_2(\alpha) = C_0\alpha^2 + C_1\alpha + C_2 \tag{16}$$

With the inclusion of the boundary conditions, the matrices $C's$ become square matrices of order 5x(N+1). A linear companion matrix method[23] is used to linearize the lambda matrix. The resulting algebraic eigenvalue problem can be written as,

$$\left\{ \begin{pmatrix} -C_0{}^{-1}C_1 & -C_0{}^{-1}C_2 \\ \mathrm{I} & 0 \end{pmatrix} - \alpha \begin{pmatrix} \mathrm{I} & 0 \\ 0 & \mathrm{I} \end{pmatrix} \right\} \begin{pmatrix} \alpha \tilde{f} \\ \tilde{f} \end{pmatrix} = 0 \tag{17}$$

The eigenvalue problem has been solved by using the subroutine ZGEEV of LAPACK.

For the vertical vorticity equation, the system of equations can be written as

$$\mathrm{D}_2(\alpha)\,\eta = 0 \tag{18}$$

The eigenvalue problem can be solved by using the procedure outlined above.

The resonance in the stability problem occurs when there is a set of parameters (α, β, ω) for which the solution of equations (2) and (4) exist for given distributions of the mean velocity and temperature, and the Reynolds number. To locate the resonance mode, the following equations are solved,

$$c_r^{CME}(\alpha, \beta, M, \mathrm{Re}) = c_r^{VV}(\alpha, \beta, M, \mathrm{Re}) \tag{19a}$$

$$c_i^{CME}(\alpha, \beta, M, \mathrm{Re}) = c_i^{VV}(\alpha, \beta, M, \mathrm{Re}) \tag{19b}$$

where c_r and c_i denote the real and the imaginary parts of the complex wave speed *c*, respectively.

The eigenvector associated with the bursting modes can be obtained by using an inverse iteration method[23],

$$\mathrm{D}_2\,\tilde{f} = \alpha \tilde{f} \tag{20}$$

In the following section, results of the validation of the numerical tools are first described. The predictions of bursting frequency in compressible turbulent boundary layers of different Mach numbers and Reynolds numbers are presented.

4.0 Results

Validation

The linear stability problems of equations (2) and (4) have been solved using the Chebyshev collocation method. To validate the numerical solver developed for this study, the linear stability results for incompressible and compressible boundary layers have been computed and compared with previous results. Comparisons are shown in Figures 1, 2 and Tables 1, 2.

First, an analytical velocity profile,

$$U = 2Y^2 - 2Y^3 + Y^4 \tag{21}$$

has been assumed, where $Y = y/\delta$. δ denotes the boundary layer thickness. The use of equation (17) allows a direct validation of the numerical solver developed in the current study of compressible boundary layers with that used for the incompressible cases.[12] The temperature distribution can be related to the velocity profile through the energy equation. The results can be written as,

$$T = T_r \{ r + (1-r)U - (1 - \frac{1}{T_r})U^2 \} \tag{22}$$

where T_r denotes the wall recover temperature and r the recovery factor ($= T_w / T_r$). For the present validation, the free stream Mach number was set at 0.001.

Figure 1 shows the calculated wave speed spectrum of equation (2) for a plane mode of Re_δ =8,000 and $\omega = 0.2354$. The complex wave speed spectra obtained by using the Chebyshev collocation method are given for various grid numbers. The result obtained by the incompressible BURFIT code has also been included for comparison. The Chebyshev collocation method shows a very good prediction of the discrete spectrum with only 41 grid points. The continuous part of the spectrum is also seen to approach that from the incompressible code as the number of grid points increases.

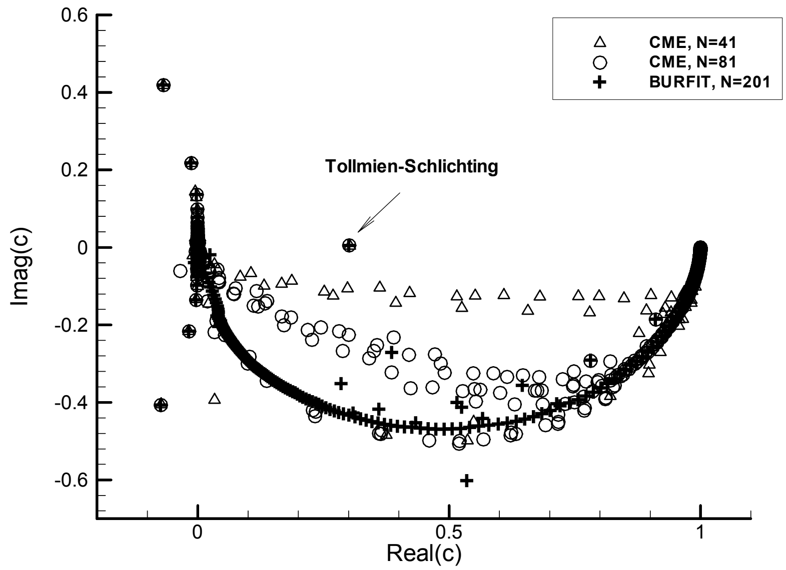

Figure 1. Complex wave speed of equation (2), polynomial velocity profile.

As can be seen in Figure 2, for the free mode of the vertical vorticity equation, the discrete spectrum is also resolved quite well for N=81 and the continuous part of the spectrum overlaps that of the incompressible result for N=201.

Table 1 shows a comparison of the calculated eigenvalues for the Blasius boundary layer with Re=1,000, $\omega = 0.07$, and $\beta = 0.12$. The calculated discrete modes obtained by using various numbers of grid points are compared with previously published data.[25] There is a good agreement between the current calculations and the data, particularly for cases with a high number of grid points N. Table 2 shows a comparison of the calculated eigenvalues for a M=4.5 supersonic boundary layer.[18] The present results obtained with N=121 agree well those obtained by using the different numerical methods.[18,21]

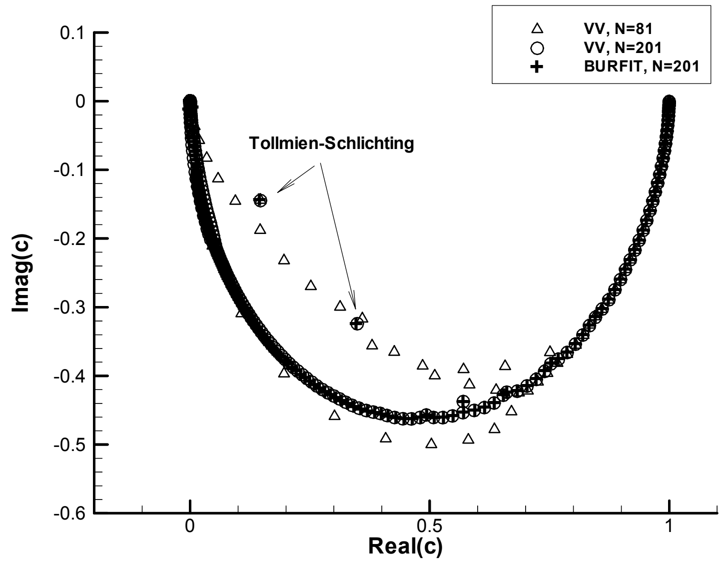

Figure 2. Complex wave speed of equation (4), polynomial velocity profile.

Table 1. Comparison of the calculated eigenvalues for the Blasius boundary layer with Re=1,000, $\omega = 0.07$, and $\beta = 0.12$.

$\alpha = 0.19861, -0.00420)$ [24]

N	α
21	(0.199086, −0.00242427)
41	(0.198624, −0.00420748)
81	(0.198611, −0.00420091)
201	(0.198610, −0.00420033)
301	(0.198610, −0.00420001)

Table 2. Comparison of the calculated eigenvalues for the supersonic boundary layer of M=4.5[18] Re=1,500, $\omega = 0.23$, and $\beta = 0.$, 4CD: fourth-order compact difference, MDSP:multi-domain spectral collocation, 4CTD: fourth-order central difference.

Present	(0.253406, −0.00249213)
Malik[18] MDSP 4CD	(0.2534048, −0.0024921) (0.2534081, −0.0024932)
Chang[21] 4CTD	(0.253469, −0.00249491)

Bursting Frequency Predictions

For an incompressible turbulent boundary layer with Re of 1,000, the bursting frequency $\omega^+ (= \omega^* \upsilon / u_\tau^2)$ has been found to be 0.0962.[12] ω^*, υ and u_τ denote the frequency, kinematic viscosity and the friction velocity, respectively. Figure 3 shows the calculated eigenvalue spectrum at this resonance condition using the current solver. For comparison with the incompressible result, the temperature profile

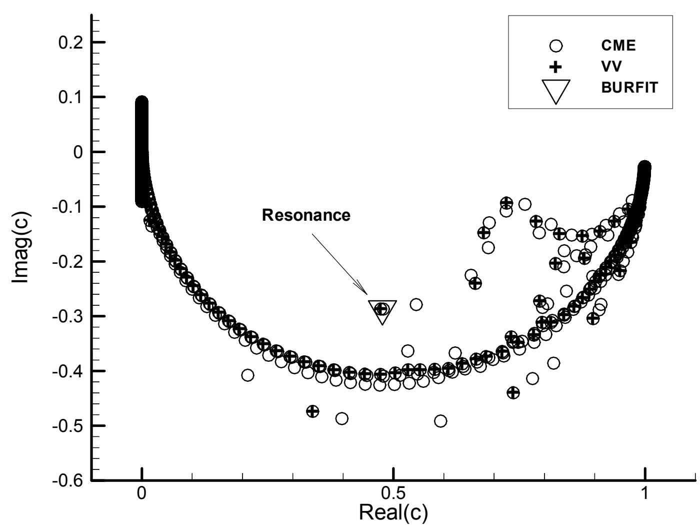

Figure 3. Complex wave speed at resonance in an incompressible turbulent boundary layer.

has been set uniform. An overlap of a discrete mode for the CME and the VV equations can be clearly identified and the overlapped mode is in a good agreement with the resonance mode obtained by using the incompressible solver BURFIT.

To identify a resonance mode for compressible boundary layers, equations (2) and (4) are first solved. Resonance occurs when the solution to the resonance condition, equation (19), is found. Equation (19) is nonlinear in its parameters and the solution involves an iteration process. A LAPACK routine HYBRD is used to solve equation (19).

The compressible turbulent boundary layers studied here have been extensively examined and documented[26-28] and are appropriate to use in the present study. The surveyed station has a Reynolds number, based on the displacement thickness of 0.0063 m, of 421,247. The associated eigenvalue spectra of equations (2) and (4) are shown in Figure 4, where the values of ω and β used have been determined by a viscous scaling of the ω^{+} and β^{+} of the incompressible resonance mode. Figure 4 shows that the eigenvalue spectra of equations (2) and (4) consist of multiple discrete, damped modes and none of the

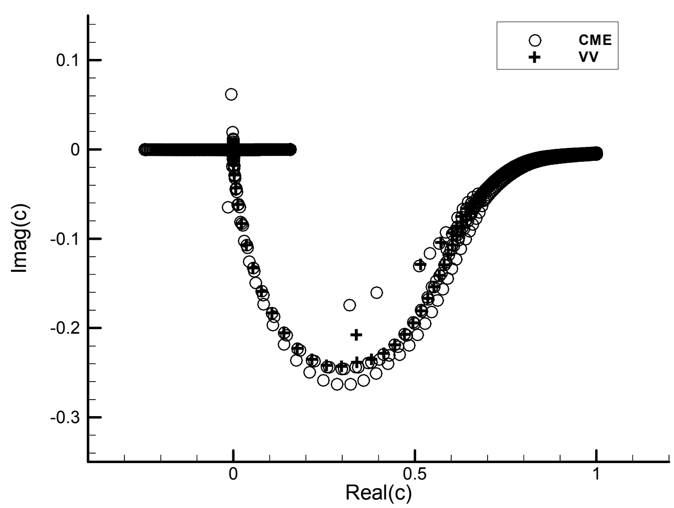

Figure 4. Wave speed spectra of the compressible turbulent boundary layer, M=2.85, Re=421,247, $\omega = 8.2706$.

discrete modes satisfies equation (19), which, according to the direct resonance model, identifies the bursting frequency. The result indicates that the near-wall viscous scaling is not appropriate for correlating the bursting frequency in incompressible turbulent boundary layers with that in the compressible turbulent boundary layer studied here. Note that since the asymptotic forms of both equations at the far field admit oscillatory, decaying solutions, there is an overlap of the continuous part of the spectra[22,29] for all frequencies. This overlap of the continuous spectra is not considered in solving equation (19) in the present study.

To locate the bursting frequency in the supersonic boundary layers, equations (2), (4) and (19) were solved as described above. In this study, possibilities for resonance to occur to the least damped mode with the lowest wave speed were examined. It can be argued that this is the mode that is most likely to be involved in a resonance. The iteration or the search for the resonance mode has been performed by solving equations (2), (4) and, (19) at every iteration step. Due to the nonlinear nature of equation (19), the process is time-consuming, especially when the initial values of ω and β have not been set appropriately. In this study, the iteration is considered complete when the L_2 norm of the residual of equation (19) has dropped below 10^{-2}. Figure 5 shows a typical history of convergence, which takes nearly 50 iterations to complete.

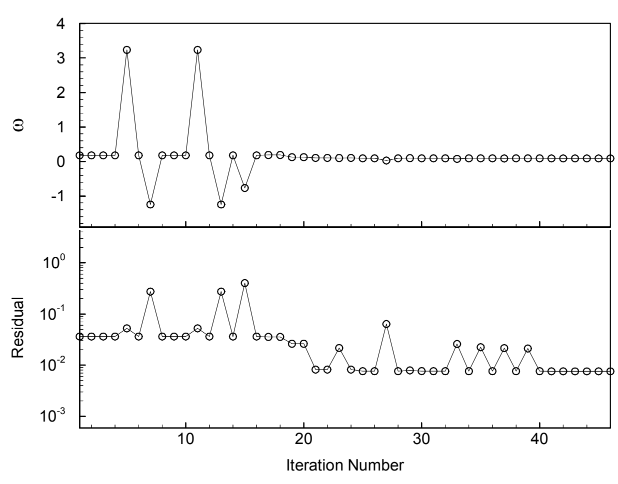

Figure 5. History of convergence. M=4, Re=421,247.

For the supersonic boundary layer of Mach number 2.85 and the Reynolds number of 421,247, two bursting frequencies have been identified. The values of ω are 0.104 (frequency 1) and 0.659 (frequency 2), respectively. The corresponding dimensional frequencies are 1.515 kHz for frequency 1 and 9.605 kHz for frequency 2. Their eigenvalue spectra are shown in Figures 6 and 7. The wave speed associated with frequency 2 is located closer to the continuous part of its spectrum than that of frequency 1. Note that the number of grid points used is 170 and the computed eigenvalues do not change in any significant way with reasonable changes in other parameters, such as the value of s_p and the size of the computational domain. The results presented in Figures 6 and 7 and in the following have been obtained with s_p =0.5. Attempts have also been made to find solutions of equation (19) based on the other discrete modes. These searches failed to identify any additional bursting frequencies.

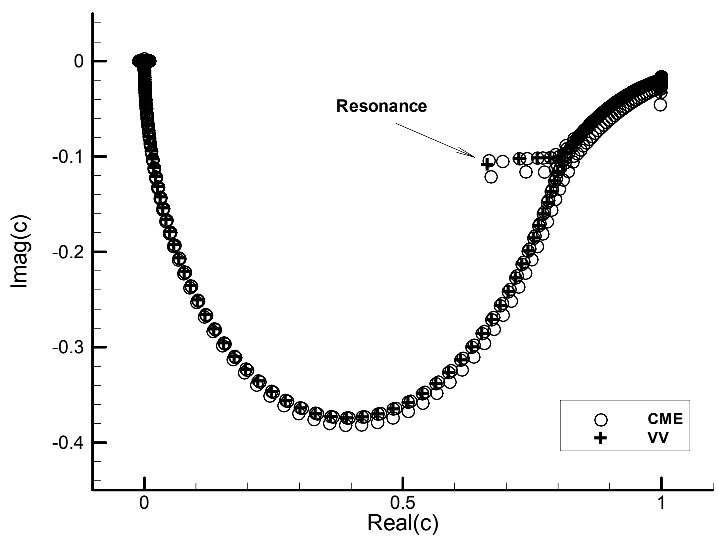

Figure 6. Wave speed spectra at bursting frequency 1 in the compressible turbulent boundary layer, M=2.85, Re=421,247, $\omega = 0.104$.

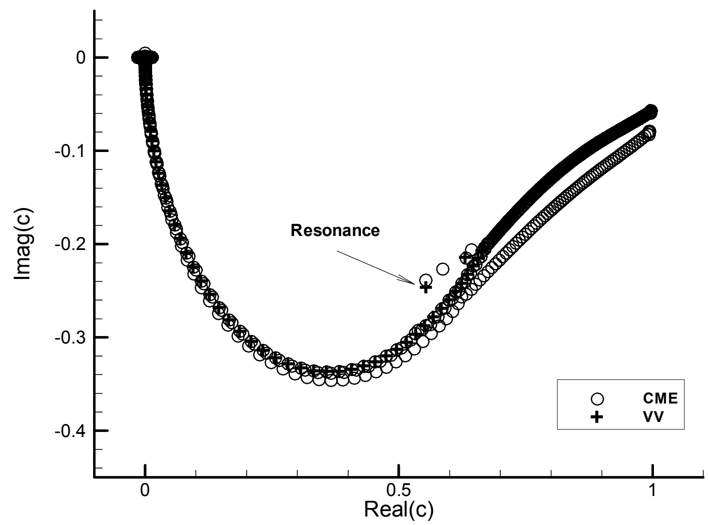

Figure 7. Wave speed spectra at bursting frequency 2 in the compressible turbulent boundary layer, M=2.85, Re=421,247, $\omega = 0.659$.

The effect of the Reynolds number on the bursting frequency predictions is shown in Figure 8.

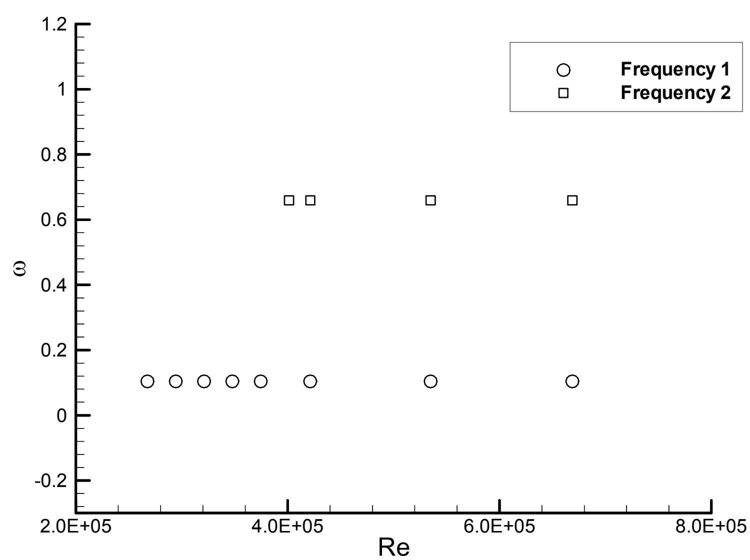

Figure 8. Bursting frequencies in the compressible turbulent boundary layers, M=2.85.

For all the Reynolds numbers calculated, ranging between 267,475 and 668,689, the low frequency of 0.104 satisfies the resonance condition. It appears to be not sensitive at all to the changes in the Reynolds number. The high bursting frequency (frequency 2) identified for Re=421,247 has also been found to satisfy the resonance condition and its value insensitive to the variation of the Reynolds number. This is true, however, only for large Reynolds numbers, in this case, higher than 401,216. For boundary layers of lower Reynolds numbers, the iteration procedure described above has not identified a converged solution near frequency 2 (ω=0.659). For example, the eigenvalue spectra for Re=374,466 at frequency 2 are shown in Figure 9. Neither the spectrum of equation (2) nor that of equation (4) appears to have any

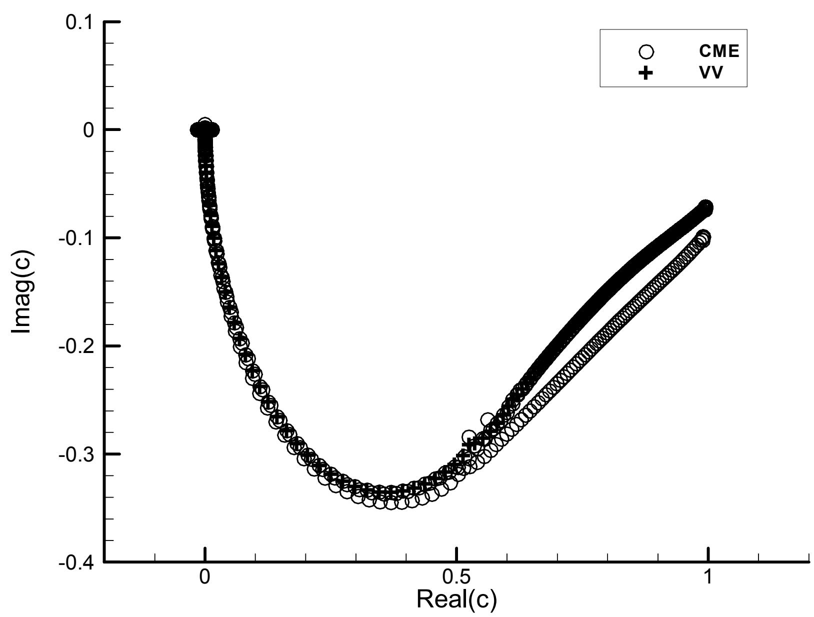

Figure 9. Complex wave speed spectra for a compressible turbulent boundary layer, M=2.85, Re=374,466.

discrete mode that can be identified with ease. Figure 10 shows the variation of ω^+ with the Reynolds numbers. A gradual decrease with the Reynolds number can be observed for both frequencies. Overall, the values of ω^+ for the compressible cases tested are one order of magnitude smaller than that in incompressible turbulent boundary layers,[12] mainly due to the high skin friction velocities.

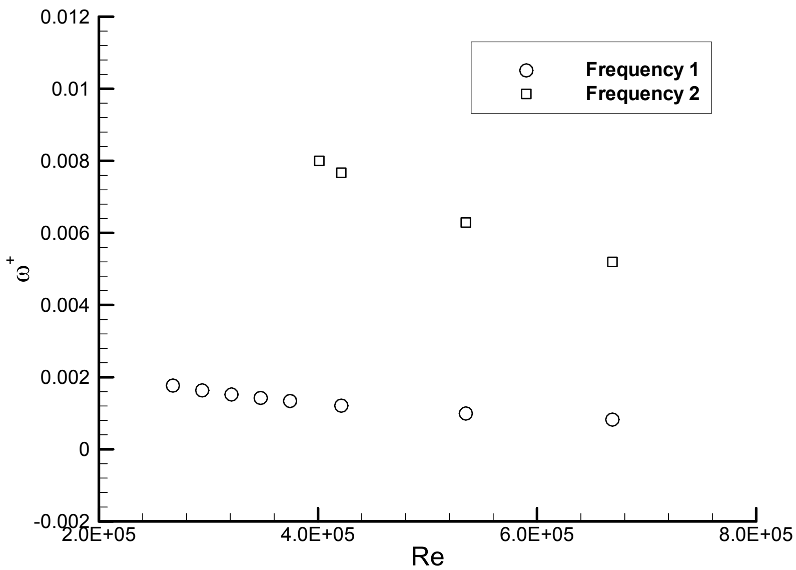

Figure 10. Bursting frequency in the compressible turbulent boundary layers.

The free stream Mach number has been increased to 4.0 while keeping the Reynolds number at 421,247 by reducing the displacement thickness of the boundary layer. The results show that frequency 1 (ω=0.104) remains a resonance frequency for this particular boundary layer. The history of convergence for this calculation has been shown in Figure 5. On the other hand, the iteration procedure did not converge to a solution that satisfied equation (19) near frequency 2. Recall that for the same Reynolds number, both frequencies have been identified as the bursting frequencies 1 and 2 in the boundary layer with a 2.85 free stream Mach number. It, then, appears that one of the two bursting frequencies does not scale with the outer time scale δ^*/U_∞.

Temperature Fluctuation Estimation

Figure 11 shows estimated profiles for the real and the imaginary parts of the temperature fluctuation for M=2.84 and Re=421,274. The bursting frequency is 0.104 (frequency I). The values of *a* and b used are set constant of 1.1/8.0 and 2.5/8.0[30] and q/U^2 is set at 0.1. The time and space coordinates are set at zero. Variations can be observed near the wall.

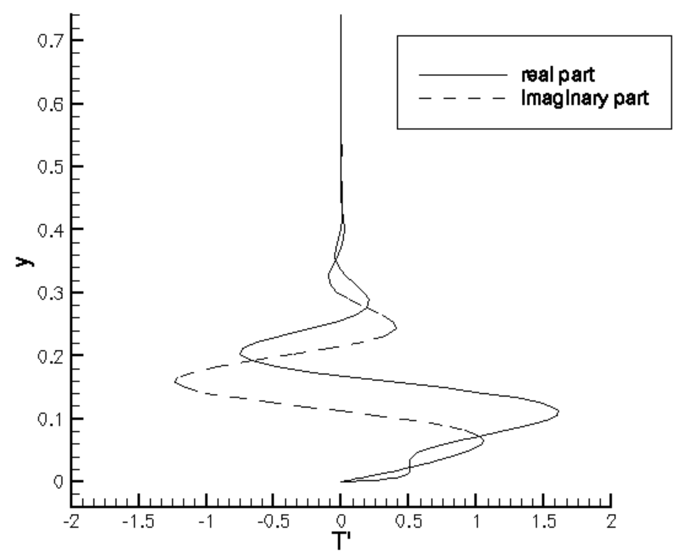

Figure 11. Temperature fluctuation. M=2.85. Re=421,274.

5. Concluding Remarks

The paper describes a computational method for the prediction of the bursting frequency in high-speed, compressible turbulent boundary layers. It is developed based on the direct resonance theory. The linear stability solver developed has been validated for the linear stability of incompressible and compressible boundary layers. The computational method has been applied to compressible boundary layers of various Reynolds numbers and Mach numbers. The results suggest possible multiple frequencies of bursting in the compressible boundary layers calculated.

Although there is evidence indicating that the computational method developed in this study for compressible boundary layers produces in satisfactory manner information obtained in a high-speed flight test, there is a need for more complete and accurate compressible experimental data to further assess the approach. Until such compressible near-wall flow structure data become available, the present computational method represents a unique way to meet the current demand for an engineering prediction capability for the bursting frequency in incompressible and compressible turbulent boundary layers. In addition, the results of this study may also serve as a guide for future experimental studies of high-speed turbulent boundary layers.

Assumptions were made in order to derive an expression for the temperature disturbance based on the local analyses. Nonlinear evolutions of the dynamics of the structures can be studied to refine the estimates.

Real gas effects at high speeds and other phenomena such as ionization can also be included.

This Page Intentionally Blank

References

1. Robinson, S., “Coherent motions in the turbulent boundary layer,” *Annu. Rev. Fluid Mech*., 23, 601-639 (1991).

2. Spina, E.F., Smits, A.J., Robinson, S.K., “The physics of supersonic turbulent boundary layers,” *Annu. Rev. Fluid Mech*., 26, 287-319 (1994).

3. Kline, S.J., Reynolds, W.C., Schraub, F.A., and Runstadler, P.W., “The structure of turbulent boundary layers,” *J. Fluid Mech.*, 30, 741-773 (1967).

4. Runstadler, P.W., Kline, S.J. & Reynolds, W.C., *An experimental investigation of flow structure of the turbulent boundary layer*, Mechanical Engineering Department, Stanford University Report MD-8 (1963).

5. Kim, H.T., Kline, S.J., and Reynolds, W.C., “The production of turbulence near a smooth wall in a turbulent boundary layer,” *J. Fluid Mech*., 50, 133-160 (1971).

6. McComb, W.D., *The Physics of Fluid Turbulence*, Clarendon Press, Oxford (2000).

7. Klebanoff, P.S., *Characteristics of turbulence in a boundary layer with zero pressure gradient*, NACA Report 1247 (1955).

8. Jang, P.S., Benny, D.J., and Gran, R.L. “On the origin of streamwise vortices in a turbulent boundary layer,” *J. Fluid Mech*., 169 (1986).

9. Zhang, Z., A and Lilley, G.M., “A theoretical model of the coherent structure of the turbulent boundary layer in zero pressure gradient”, *Turbulent Shear Flows 3*, Ed. L.J.S. Bradbury, F. Durst, B.E. Launder, F.W. Schmidt, J.H. Whitelaw, Springer (1981).

10. Zhou, H. and Luo, J.-S., “Theoretical models for the coherent structures in a turbulent boundary layer,” *Near-Wall Turbulent Flows*, Ed. R.M.C. So, C.G. Speziale and B.E. Launder, Elsevier Science Publishers (1993).

11. Morrison, W.R.B. and Kronauer, R.E., “Structural similarity for fully developed turbulence in smooth tubes,” *J. Fluid Mech*., 39 (1969).

12. Liou, W.W., Fang, Y, and Baty, R.S., “Global numerical prediction of bursting frequency in turbulent boundary layer,” *Int. J. Num. Meth. Heat & Fluid Flow*, 10 (2000).

13. Liou, W.W. and Morris, P.J., “Weakly nonlinear models for turbulent mixing in a plane mixing layer,” *Phys. Fluids*, 4 (1992).

14. Morkovin, M.V., “Effects of compressibility on turbulent flows,” *Mechanique de la Turbulence*, Ed. A. Favre., 367-380 (1962).

15. Lees, L, and Lin, C.C., *Investigation of the stability of the laminar boundary layer in a compressible fluid*, NACA TN 1115 (1946).

16. Mack, L.M., *Boundary layer linear stability theory*, AGARD Report No. 709 (1984).

17. Liou, W.W., Huang, G., Shih, T.-H., "Turbulence model assessment of shock wave/turbulent boundary-layer interaction in transonic and supersonic flows," *Computers and Fluids*, 29, 275-299 (2000).

18. Malik, M.R., "Numerical methods for hypersonic boundary layer stability," *J. Comp. Physics*, 86, 376-413 (1990).

19. Joslin, R.D., Morris, P.J. and Carpenter, P.W., "The role of three-dimensional instabilities in compliant-wall boundary layer transition," *AIAA J.*, 29, 1603-1610 (1991).

20. Chang, C.-L. and Malik, M.R., "Oblique-mode breakdown and secondary instability in supersonic boundary layers," *J. Fluid Mech*.,273, 323-360 (1994).

21. Chang, C.-L., *The Langley stability and transition analysis codes (LASTRAC) – Part I: LST, linear & nonlinear PSE for 2D, asixymmetric and infinite swept wing boundary layers*, NASA TM, in preparation, 2002.

22. Liou, W.W. and Morris, P.J., "The eigenvalue spectrum of the Rayleigh equation for a plane shear layer," *Int. J. Num. Meth. Fluids*, 15, 1407 (1992).

23. Bridges, T.J. and Morris, P.J., "Differential eigenvalue problems in which the parameter appear nonlinearly," *J. Computational Physics*, 55, 437 (1984).

24. Canuto, C., Hussaini, M.Y., Quarteroni, A. and Zang, T.A. Etd., *Spectral Method in Fluid Dynamics*, Springer-Verlag (1987).

25. Bridges, T.J. and Morris, P.J., "Boundary layer stability calculations," *Phys. Fluids*, 30, 3351-3358 (1987).

26. Spina, E.F. and Smits, A.J., "Organized structures in a compressible, turbulent boundary layer," *J. Fluid Mech*., 182, 85-100 (1987).

27. Settles, G.S. and Dodson, L.J., *Hypersonic shock/boundary layer interaction database*, NASA CR 177577 (1991).

28. Fernholz, H.H., Dussauge, J.P., Finley, P.J., and Smits, A.J., *A survey of measurements and measuring techniques in rapidly distorted compressible turbulent boundary layers*, AGARDograph No. 315 (1989).

29. Grosch, C.E. and Salwen, H., "The continuous spectrum of the Orr-Sommerfeld equation. Part I. The spectrum and the eigenfunctions," *J. Fluid Mech*., 87, 33 (1978).

30. Smits, A.J. and Dussauge, J.-P., *Turbulent Shear Layers in Supersonic Flow*, AIP Press (1996).

Distribution

10	William W. Liou, Ph.D. Department of Mecahnical and Aeronautical Engineering 2065 Kohrman Hall Western Michigan University Kalamazoo, MI 49008		
10	Yichuan Fang Department of Mecahnical and Aeronautical Engineering 2065 Kohrman Hall Western Michigan University Kalamazoo, MI 49008		
3	MS-0482	R. S. Baty	2131
1	MS 0529	K. W. Sorensen	2343
3	MS 0529	B. C. Brock	2343
1	MS-0537	D. R. Weiss	2333
1	MS-0537	S. C. Holswade	2333
1	MS-0824	A. C. Ratzel	9110
3	MS-0825	D. L. Potter	9115
1	MS-0825	C. J. Roy	9115
1	MS-1174	W. H. Rutledge	15414
1	MS 0612	Review & Approval Desk for DOE/OSTI	9612
2	MS 0899	Technical Library	9616
1	MS 9018	Central Technical Files	8945-1